Analysis of ^{31}P MAS NMR Spectra and Transversal Relaxation of Bacteriophage M13 and Tobacco Mosaic Virus

Pieter C. M. M. Magusin and Marcus A. Hemminga
From the Department of Molecular Physics, Agricultural University, Dreijenlaan 3, 6703 HA Wageningen, The Netherlands

ABSTRACT Phosphorus magic angle spinning nuclear magnetic resonance (NMR) spectra and transversal relaxation of M13 and TMV are analyzed by use of a model, which includes both local backbone motions of the encapsulated nucleic acid molecules and overall rotational diffusion of the rod-shaped virions about their length axis. Backbone motions influence the sideband intensities by causing a fast restricted reorientation of the phosphodiesters. To evaluate their influence on the observed sideband patterns, we extend the model that we used previously to analyze nonspinning ^{31}P NMR lineshapes (Magusin, P.C.M.M., and M. A. Hemminga. 1993a. *Biophys. J.* 64:1861–1868) to magic angle spinning NMR experiments. Backbone motions also influence the conformation of the phosphodiesters, causing conformational averaging of the isotropic chemical shift, which offers a possible explanation for the various linewidths of the centerband and the sidebands observed for M13 gels under various conditions. The change of the experimental lineshape of M13 as a function of temperature and hydration is interpreted in terms of fast restricted fluctuation of the dihedral angles between the POC and the OCH planes on both sides of the ^{31}P nucleus in the nucleic acid backbone. Backbone motions also seem to be the main cause of transversal relaxation measured at spinning rates of 4 kHz or higher. At spinning rates less than 2 kHz, transversal relaxation is significantly faster. This effect is assigned to slow, overall rotation of the rod-shaped M13 phage about its length axis. Equations are derived to simulate the observed dependence of T_{2e} on the spinning rate.

INTRODUCTION

Although the protein coats of both bacteriophage M13 and tobacco mosaic virus (TMV) are highly regular cylindrical arrays of rigidly fixed protein monomers, the packing of the viral genome within the virions is completely different. From x-ray studies, much information is obtained about the structure and the interactions of the single-stranded RNA molecule in TMV, which is buried within the coat between layers of subunits, following the protein helix with three nucleotides per protein subunit at a radius of about 40 Å (Stubbs et al., 1977). In contrast, much less is known about the geometry of the circular, single-stranded DNA molecule in M13, which is probably located along the inside of the tubular protein coat. Phosphorus nuclear magnetic resonance (NMR) studies have indicated that the DNA molecule is immobilized (DiVerdi and Opella, 1981), presumably due to electrostatic interaction between the negatively charged phosphodiesters of the nucleic acid backbone and positively charged lysine residues of the protein coat. The interaction with the highly regular protein coat, however, does not seem to force the DNA backbone into some regular structure, because a large variety of crystallographic and spectroscopic techniques have been unable to reveal such regularity (Marvin et al., 1974; Banner et al., 1981; Thomas et al., 1988; Cross et al., 1983b). Because phosphorus nuclei in M13 and TMV are only present in the phosphodiesters of the encapsulated nucleic acid molecules, ^{31}P NMR spectroscopy can be used to study structure and dynamics of the nucleic acid backbone selectively. Motional lineshape narrowing and transversal relaxation observed in ^{31}P NMR studies of virus gels can neither be explained by (restricted) overall rotation of the virus particles as rigid rods about their length axis, nor by isotropic motion of the phosphodiesters inside (Magusin and Hemminga, 1993a). Instead, a combined diffusion model with fast restricted motions of the encapsulated nucleic acid dominating the spectrum superimposed on slow overall rotation of the virions affecting transversal relaxation provides a consistent picture. Simulation of the nonspinning ^{31}P NMR lineshape of TMV is greatly improved by the assumption that one of the three binding sites is more mobile than the other two. However, unambiguous assignment of motional amplitudes to specific binding sites is not possible, because their powder lineshapes strongly overlap.

The problem of overlapping resonances may be solved by employing magic angle spinning (MAS), which breaks up a broad ^{31}P NMR powder lineshape into a sharp centerband at the isotropic chemical shift position flanked by rotational sidebands. The relative intensities of these sidebands have been calculated for the "ideal" case that the orientations of the chemical shift tensors in the sample are rigidly fixed with respect to the rotor (Herzfeld and Berger, 1980). Motions, however, may cause "anomalous" MAS behavior and, in fact, motional information may be extracted from anomalous features (Schmidt et al., 1986; Schmidt and Vega, 1987). Resonances are more easily resolved and specific sideband patterns, including their motional information, may be assigned to specific isotropic chemical shifts, because for phosphodiester compounds, the width of the centerband and the sidebands is typically a few parts per million. Assignment of isotropic chemical shifts, in turn, is facilitated by the strong

Received for publication 13 April 1993 and in final form 25 January 1994.
Address reprint requests to Dr. Hemminga, the Department of Molecular Physics, Agricultural University, P.O. Box 8128, 6700 ET Wageningen, The Netherlands.

0006-3495/94/04/1197/12 $2.00

dependence of the isotropic chemical shift on the conformation of the phosphodiester group (Gorenstein, 1981; Giessner-Prettre et al., 1984). Resonances of inequivalent phosphodiesters in a nucleic acid molecule packed within a virion may therefore be resolved in MAS NMR spectra, if their conformations are sufficiently different. Indeed, ^{31}P MAS NMR spectra of TMV solutions (Cross et al., 1983a) and dried TMV pellets (Hemminga et al., 1987) show two resolved sideband patterns with an overall intensity ratio of approximately 2, which have been assigned by comparing torsion angle values for the three types of phosphodiesters in TMV (Hemminga et al., 1987). MAS NMR spectra of bacteriophage fd, which is closely related to M13, only contain a single, broad centerband flanked by sidebands (DiVerdi and Opella, 1981), indicating that a continuous distribution of phosphodiester conformations is present in the phage, rather than a distinguishable few.

In this paper, we will present the results of ^{31}P MAS NMR experiments applied to M13 and TMV. Anomalous sideband patterns of M13 and TMV will be analyzed in terms of restricted reorientation of the phosphodiester groups which is caused presumably by fast nucleic acid backbone motions. It will be demonstrated that the same type of restricted phosphodiester reorientation can also explain transversal ^{31}P relaxation measured at a spinning rate of 4 kHz or more. Especially for M13, a model is developed to interpret the lineshape of the centerband and the sidebands in terms of a continuous distribution of phosphodiester conformations and to calculate the narrowing effect of specific conformational fluctuations on the lineshape of the centerband and sidebands. The spinning rate dependence of the T_{2e} values measured for M13 at low spinning rates will be explained by slow, overall rotation of the rod-shaped virions about their length axis.

THEORY

Sideband intensities

To calculate the combined effect of both MAS and rotational diffusion on NMR spectra and transversal relaxation of ^{31}P in virions, the orientation of a ^{31}P chemical shift tensor is specified most conveniently by a sequence of three rotation steps, which relates the laboratory frame via subsequent axis systems fixed to the rotor and the virus particle to the principle axis system of the chemical shift tensor given by the Euler angles $\Omega = (\chi, \zeta, \xi)$, $\Omega' = (\phi, \theta, \psi)$, and $\Omega'' = (\alpha, \beta, \gamma)$, respectively. Consequently, the precession frequency ω caused by the combined Zeeman and orientation-dependent chemical shift interaction may be expressed in terms of the Wigner functions $D^2_{m'm}(\alpha\beta\gamma) = \exp(im'\gamma)d^2_{m'm}(\beta)\exp(im\alpha)$ (Edmonds, 1960; Haeberlen, 1976) as

$$\omega(\Omega, \Omega', \Omega'') = \omega_0 + \omega_0\sigma_0 + \omega_0 \sum_{m,m'=-2}^{2} D^2_{m0}(\Omega)D^2_{m'm}(\Omega') \times [F_0D^2_{0m'}(\Omega'') + F_2(D^2_{2m'}(\Omega'') + D^2_{-2m'}(\Omega''))] \quad (1)$$

where $\omega_o = \gamma B_o$ is the Zeeman angular frequency, $\sigma_o = (\sigma_{11} + \sigma_{22} + \sigma_{33})/3$, $F_0 = (\sigma_{33} - \sigma_o)$ and $F_2 = (\sigma_{22} - \sigma_{11})/\sqrt{6}$ for a chemical shift tensor with principle values σ_{11}, σ_{22}, and σ_{33}. It is assumed that, although conformational motions may cause σ_o to fluctuate, F_0 and F_2 are constant in time. This is a reasonable assumption, because the F_0 and F_2 values measured for ^{31}P in various nucleic acids, generally occur within the ranges -105 ± 10 ppm and -25 ± 2 ppm, respectively (Magusin and Hemminga, 1993a; Hemminga et al., 1987), indicating that conformationally induced changes of F_0 and F_2 are relatively small. For MAS at an angular frequency ω_r, the angles ζ and ξ in Eq. 1 are set to $\arccos(1/\sqrt{3})$ and $\omega_r t$, respectively. All virion orientations Ω' with respect to the MAS rotor equally occur in an isotropic powder and the number of relative chemical shift tensor orientations Ω'' within the virion may vary from a single one in Pf1 (Cross et al., 1983b), for example, or three in TMV (Cross et al., 1983a), for instance, to a large value representing a nucleic acid backbone without structural correlation to the viral coat geometry, such as bacteriophage fd (Cross et al., 1983b), so that the number of angles actually involved in the calculation can become quite large. Due to the symmetry properties of Eq. 1, however, only θ, β, and γ values between 0 and $\pi/2$ need to be taken into account, as long as ϕ and ψ vary between 0 and 2π, and α may be chosen 0 without loss of generality.

In our previous analysis of static ^{31}P NMR lineshapes of both viruses at 121.5 MHz, we characterized the net effect of the probably complex dynamics of the encapsulated nucleic acid molecule by a single "cumulative motional amplitude" using a simple model, in which the phosphodiesters undergo fast restricted rotation about the length axis of the virions. Extending this model to MAS NMR, we assume that the phosphodiesters undergo uniaxial diffusion restricted to angles α $[\alpha_o - \lambda, \alpha_o + \lambda]$, fast enough to allow us to replace $D^2_{nm'}(\Omega'')$in Eq. 1 by the average value $D^2_{nm'}(\Omega'')$ sinc (m'λ),where Ω'' is redefined as $(\alpha_o, \beta, \gamma)$ and sinc$(m'\lambda)$ denotes the function $\sin(m'\lambda)/m'\lambda$. After this substitution, the relative sideband intensities in the MAS NMR spectrum may be calculated by Fourier transformation of the free induction decay

$$S(t) = (8\pi^2)^{-2} \int d\Omega' \int d\Omega'' \exp\left[i \int_0^t \omega(\zeta, \omega_r, t', \Omega', \lambda, \Omega'')\, dt' \right] \quad (2)$$

with

$$\int_0^t \omega(\zeta, \omega_r, t', \Omega', \lambda, \Omega'')\, dt' = \omega_0(1 + \sigma_0)t + \omega_0 \sum_{m\neq 0} d^2_{m0}(\zeta) \frac{e^{im\omega_r t} - 1}{m\omega_r} \times \sum_{m'=-2}^{2} D^2_{m'm}(\Omega') \frac{\sin(m'\lambda)}{m'\lambda} [F_0D^2_{0m'}(\Omega'') + F_2(D^2_{2m'}(\Omega'') + D^2_{-2m'}(\Omega''))]$$

As Eq. 2 shows, a fast restricted motion reduces the apparent chemical shift anisotropy and thereby influences the sideband pattern produced by MAS.

Transversal relaxation

Slow, unrestricted rotational diffusion of the rod-shaped virions about their length axes superimposed on the fast restricted nucleic acid motions inside is incorporated in our model by adding a diffusion term $D(\partial^2/\partial\psi^2)$ to the so-called stochastic Liouville equation (SLE) (Dufourc et al., 1992). For the positive and negative-helicity components $\mu_\pm(\Omega', \Omega'', t)\, I_\pm$ of the spin density operator $\rho(\Omega', \Omega'', t)$, where I_+ and I_- are the raising and lowering operators for a spin-1/2 nucleus, the relevant part of the SLE becomes

$$\frac{d\mu_\pm(\Omega', \Omega'', t)}{dt} = \left(\pm i\omega(\Omega', \Omega'', t) + D\frac{\partial^2}{\partial\psi^2} \right) \mu_\pm(\Omega', \Omega'', t) \quad (3)$$

where the notation of $\omega(\zeta, \omega_r, t, \Omega', \lambda, \Omega'', t)$ in Eq. 2 has been simplified to $\omega(\Omega', \Omega'', t)$. Unfortunately, Eq. 3 cannot be solved analytically and some approximation must be made. Theoretical investigation of the influence of rotational diffusion on transversal relaxation under nonspinning conditions, has shown that for very slow diffusion the relaxation rate may be much larger than the diffusion coefficient (Magusin and Hemminga, 1993b). In such cases, most spin density stays close to its initial orientation within times comparable with the transversal relaxation time. This allows local, linear approximations to be made for the chemical shift as a function of the ori-

entation, which greatly facilitates the calculation of transversal relaxation. We have employed the same method to approximately solve Eq. 3 for very slow diffusion. For every orientation $\Omega'_o = (\phi, \theta, \psi_o)$, $\omega(\Omega', \Omega'', t)$ is locally approximated as $\omega(\Omega'_o, \Omega'', t) + \omega'(\Omega'_o, \Omega'', t)(\psi - \psi_o)$, where $\omega'(\Omega'_o, \Omega'', t)$ denotes the derivative $\partial\omega/\partial\psi$ for $\psi = \psi_o$. With this linear approximation, the two spin density components can be obtained analytically from Eq. 3. Similar to the derivation of transversal relaxation for spins diffusing in a static field gradient (Slichter, 1978), it follows that a π pulse at $t = \tau$ produces an echo at $t = 2\tau$ given by

$$E(2\tau) = (8\pi^2)^{-2} \int d\Omega' \int d\Omega'' \exp\left[-2D \int_0^\tau \left\{ \int_0^t \omega'(\Omega', \Omega'', t')\, dt' \right\}^2 dt \right] \quad (4)$$

where Ω' has been redefined as Ω'_o. When the refocussing π pulse is given at $t = nT_r$, i.e., after an integral number of spinner rotations, the oscillating terms in the argument of the exponential function in Eq. 4 vanish and only terms linear in t remain

$$E(2nT_r) = (8\pi^2)^{-2} \int d\Omega' \int d\Omega'' \exp\left[-D \frac{\omega_0^2}{\omega_r^2} 2nT_r a(\Omega', \Omega'') \right] \quad (5)$$

where

$$\begin{aligned} a(\Omega', \Omega'') = \Bigg\{ & \left[\sum_{m\neq 0} d^2_{m0}(\zeta) \frac{1}{m} \sum_{m'\neq 0} D^2_{m'm}(\Omega'_0) \frac{\sin(m'\lambda)}{\lambda} \right. \\ & \left. \times [F_0 D^2_{0m'}(\Omega'') + F_2(D^2_{2m'}(\Omega'') + D^2_{-2m'}(\Omega''))] \right]^2 \\ & - \sum_{m\neq 0} d^2_{m0}(\zeta) d^2_{-m0}(\zeta) \frac{1}{m^2} \sum_{m'\neq 0} D^2_{m'm}(\Omega'_0) \frac{\sin(m'\lambda)}{\lambda} \\ & \times [F_0 D^2_{0m'}(\Omega'') + F_2(D^2_{2m'}(\Omega'') + D^2_{-2m'}(\Omega''))] \\ & \times \sum_{m'\neq 0} D^2_{m'-m}(\Omega'_0) \frac{\sin(m'\lambda)}{\lambda} \\ & \times [F_0 D^2_{0m'}(\Omega'') + F_2(D^2_{2m'}(\Omega'') + D^2_{-2m'}(\Omega''))] \Bigg\} \end{aligned}$$

Eq. 5 can be used to calculate the decay of echoes numerically. In practice, however, this multiexponential relaxation is hard to distinguish from a single exponential. An apparent relaxation time T_{2e}^{SOR} due to the slow overall rotation (SOR) of the virions, may be defined from the apparent derivative of Eq. 5 at $nT_r = 0$, which can be derived by use of the orthogonal properties of the second rank Wigner functions as

$$\frac{1}{T_{2e}^{SOR}} = D \frac{M_2}{\omega_r^2} \left\{ \frac{1}{5} \mathrm{sinc}^2(\lambda) + \frac{4}{5} \mathrm{sinc}^2(2\lambda) \right\} \quad (6)$$

where M_2 denotes the second moment of the nonspinning lineshape in the absence of backbone motions, given by $\omega_0^2(F_0^2 + 2F_2^2)/5$. For extremely slow motion, a similar equation may be derived for T_2 effects caused by homonuclear dipolar fluctuations in MAS experiments (Mehring, 1983). As follows from Eq. 6, on the one hand, T_{2e}^{SOR} decreases as the slow overall rotation becomes faster and as M_2 becomes larger at increasing magnetic field strength. On the other hand, T_{2e}^{SOR} increases at increasing amplitude λ of the backbone motions and at increasing spinning rate ω_r. At high spinning rates, therefore, other relaxation mechanisms, which are independent of the spinning rate, become more important. The same fast backbone motions that modify the sideband intensities (Eq. 2) and suppress the relaxation effect caused by slow overall rotation (Eq. 6), also induce transversal relaxation by causing local field fluctuations due to the chemical shift anisotropy (CSA) of the ^{31}P nuclei. From the general formula $1/T_{2e} \approx \Delta M_2\, \tau$, which relates T_{2e} to the portion of the second moment ΔM_2 modulated by motion with a short correlation time τ (Pauls et al., 1985), we previously derived for fast restricted uniaxial diffusion about the length axis of the virus particle an approximate contribution $1/T_{2e}^{CSA}$ to the transversal relaxation rate under nonspinning conditions as (Magusin and Hemminga, 1993b)

$$\frac{1}{T_{2e}^{CSA}} = \frac{M_2\{2 - \mathrm{sinc}^2(\lambda) - \mathrm{sinc}^2(2\lambda)\}}{15D'} \quad (7)$$

where the diffusion coefficient D' may be regarded as an effective measure of the rate of backbone motions. If the backbone motions are much faster than the spinning rate (10^3 Hz), their influence on transversal relaxation is hardly modified by MAS, and Eq. 7 is still approximately valid under spinning conditions. In contrast to T_{2e}^{SOR}, T_{2e}^{CSA} increases as the motion becomes faster and decreases as the amplitude λ becomes larger. This is a consequence of the fact that the backbone motions are assumed to be fast, as compared with the nonspinning linewidth in the absence of backbone motion, and that the portion of the second moment that is modulated by the backbone motion increases as the motional amplitudes become larger. Similar to T_{2e}^{SOR}, T_{2e}^{CSA} is inversely proportional to the square of the resonance frequency ω_o. In our previous analysis of transversal ^{31}P relaxation of nonspinning samples (Magusin and Hemminga, 1993a), we have assumed that $T_{2e}^{CSA} \gg T_{2e}^{SOR}$ so that it may be neglected. In contrast, it will be shown in this paper that T_{2e}^{SOR} is negligible at spinning rates of 4 kHz or higher. At intermediate spinning rates, the total transversal relaxation time T_{2e} is given by

$$\frac{1}{T_{2e}} = \frac{1}{T_{2e}^{SOR}} + \frac{1}{T_{2e}^{CSA}} \quad (8)$$

Lineshape of the centerband and the sidebands

To simulate a finite linewidth for the centerband and the sidebands, Eq. 2 must still be multiplied by some slowly decaying function representing the effect of inhomogeneous and homogeneous line broadening. For this purpose, one could use a simple gaussian or exponential decay, selected by fitting calculated spectra to the experimental spectrum. Such a procedure, however, does not explain the observed lineshape of the centerband and the sidebands, and changes thereof under various conditions. Therefore, a model is set up here, especially for M13, which relates the lineshape to a continuous distribution of phosphodiester conformations and transversal relaxation. It further demonstrates how conformational fluctuations may influence the linewidth.

A strong correlation has been found between the isotropic chemical shift σ_o and the RO-P-OR′ bond angle Φ, which typically varies in the range 102° ± 3° for different nucleic acid molecules (Giessner-Prettre et al., 1984). Because the backbone of M13 DNA is probably disordered, values of Φ in our model are distributed in a range around some central value Φ_o, which could be, e.g., 102°, according to the density function $P_w(\Phi - \Phi_o) = \exp[-\{(\Phi - \Phi_o)/w\}^2]$, where w determines the distribution width. In this range σ_o is a linear function of Φ, $\sigma_o(\Phi) = G(\Phi - \Phi_o)$ with $G \approx -2$ ppm per degree (Gorenstein, 1981). Ab initio calculations have indicated that the isotropic chemical shift σ_o of the ^{31}P nucleus in the dimethyl phosphate anion also strongly depends on the two smallest dihedral angles θ_1 and θ_2 on both sides of the ^{31}P nucleus between the respective POC and OCH planes (Giessner-Prettre et al., 1984). Effects on σ_o caused by simultaneous variation of both angles are simply additive. The graphic representation of σ_o versus θ_1 or θ_2 shows a 120°-periodic, roughly sinusoidal dependence on each angle, whereby σ_o shifts approximately 3.5 ppm upfield as θ_1 or θ_2 increases from 0° to 60°. We therefore assume in our model for the phosphodiesters in the DNA molecule encapsulated in M13, that the static contribution of the two dihedral angles to the isotropic ^{31}P shift is $b \sin\{3(\theta_\kappa - \theta_o)\}$ each, where $\theta_o = 30°$ and b is a fitting parameter roughly equal to −1.75 ppm. In addition, because the absolute values of θ_1 and θ_2 typically vary in a range 35° ± 20° for different nucleic acid helices (Giessner-Prettre et al., 1984) and the geometry of the M13 DNA backbone seems to be irregular, we take values for θ_1 and θ_2 symmetrically distributed according to the density function $P_v(\theta_\kappa - \theta_o) = \exp[-\{(\theta_\kappa - \theta_o)/v\}^2]$, where $\theta_o = 30°$ (causing symmetric lineshapes) and $v = 20°$ (as a realistic

distribution width). To include the effect of conformational fluctuations into the model as well, we further assume that the dihedral angles θ_κ are not rigidly fixed, but fluctuate very rapidly between a lower value $\langle\theta_\kappa\rangle - \mu$ and an upper value $\langle\theta_\kappa\rangle + \mu$, so that the contribution to σ_o is scaled to the time-average $b \sin\{3(\langle\theta_\kappa\rangle - \theta_o)\}\ \mathrm{sinc}(3\mu)$, where the sinc function is as defined before Eq. 2. Taking both bond angle and dihedral angle effects into account and adding to this the transversal relaxation caused by slow overall motion and fast backbone motion (Eq. 8), we calculate the lineshape of the centerband and the sidebands by Fourier transformation of the free induction decay defined at integer multiples of the spinner rotation time by

$$S(nT_r) = \exp\left[-\frac{nT_r}{T_{2e}}\right] \int P_w(\Phi)\exp[iGw\Phi nT_r]\,d\Phi \times \int P_v(\theta_1)\exp[ib\sin(3\theta_1)\mathrm{sinc}(3\mu)nT_r]\,d\theta_1 \times \int P_v(\theta_2)\exp[ib\sin(3\theta_2)\mathrm{sinc}(3\mu)nT_r]\,d\theta_2 \quad (9)$$

where Φ, θ_1, and θ_2 have been redefined as $\Phi - \Phi_o$, $\langle\theta_1\rangle - \theta_o$, and $\langle\theta_2\rangle - \theta_o$, respectively. As Eq. 9 indicates, there is dual effect of nucleic acid backbone motions on the lineshape. On the one hand, the fluctuation of the dihedral angles caused by them tends to narrow the centerband and the sidebands in ^{31}P MAS NMR spectra. On the other hand, backbone motions also cause transversal relaxation (Eq. 7), which broadens the lineshape. In principle, the isotropic chemical shift fluctuations caused by conformational changes also contribute to transversal relaxation. This contribution, however, is presumably small as compared with relaxation by phosphodiester reorientation, because the width of the isotropic chemical shift range of a few parts per million associated with conformational inhomogeneity is much smaller than the "size" $\sigma_{33} - \sigma_{11}$ of the chemical shift anisotropy being 180 ppm for ^{31}P nuclei in phosphodiesters. The relaxation effect caused by isotropic chemical shift fluctuations is therefore assumed to be negligible.

MATERIAL AND METHODS

M13 and TMV were grown, purified, and concentrated as described previously (Magusin and Hemminga, 1993a). NMR spectra were recorded on a Bruker AM500 and a CXP300 spectrometer operating at a ^{31}P frequency of 202.5 and 121.5 MHz, respectively. The MAS experiments were conducted in standard 7-mm Bruker VT MAS-DAB probes. For M13 and TMV gels at room temperature special care had to be taken to let the samples spin. The following spinner preparation was the most successful. Zirconia spinners were carefully filled with the sticky viral material, packed by use of an Eppendorf lab centrifuge to remove air bubbles from the samples. Tightly fitting Kel-F caps were used to close the spinners, and an ink marker was used for sealing. Leakage of material or evaporation of water from the samples was checked by comparing the spinner weights before and after every experiment. It was important to clean the outside of the spinner thoroughly with alcohol to remove all traces of material. After this preparation spinners could sometimes attain spinning speeds up to 5 kHz. Stable spinning of dilute viral gels was almost impossible at concentrations less than 200 mg/ml or at temperatures more than 40°C, probably due to the high fluidity of the sample under these conditions.

Because the tuning properties of the wet virus gels were quite different as compared with the solid reference compounds commonly used to set the experimental conditions, the rf pulses were adjusted on the sample itself. In experiments at 121.5 MHz the ^{31}P $\pi/2$ pulse length was set to 5 μs and at 202.5 MHz to 8 μs. The ^{1}H decoupler field strength was measured on the sample itself by varying the length of the proton excitation pulse in a cross-polarization pulse sequence. Spectra were recorded using a Hahn echo pulse sequence to remove the effect of probe ringing on the weak signal. For recording standard MAS NMR spectra, a refocussing pulse was given after one spinner rotation. In all experiments a CYCLOPS phase alternation was used to remove the effects of pulse imperfections, and high-power proton decoupling was on during refocussing delays and acquisition time. Transversal relaxation was studied by acquiring the Hahn echoes at even multiples of the spinner rotation time. To suppress noise, the echoes were Fourier transformed, and only the relevant parts of the spectrum were integrated.

Sideband patterns, lineshapes, and transversal relaxation at high and low spinning rates were simulated utilizing Fortran and Igor programs based on the equations described under Theory. For ^{31}P NMR in M13 relative chemical shift tensor values $\sigma_{11} - \sigma_o = 77$ ppm, $\sigma_{22} - \sigma_o = 18$ ppm, and $\sigma_{33} - \sigma_o = -95$ ppm were taken (where σ_o is the isotropic shift). For TMV the values 83, 25, and -108 ppm were taken from the literature (Cross et al., 1983a). In simulations for M13 it was assumed that a random distribution of chemical shift tensor orientations exists within the phage. For TMV the orientation of ^{31}P chemical shift tensor for the three different binding sites with respect to the rod-shaped TMV was approximately derived from the ^{31}P atomic coordinates as described earlier (Magusin and Hemminga, 1993a). The best fits to the experimental sideband patterns and lineshapes of M13 and TMV were found by least square fitting, allowing height, baseline, and isotropic shift of simulated sideband patterns and lineshapes to vary. Simulated transversal relaxation curves were fitted to the experimental relaxation decays with only height as a variable.

RESULTS

MAS NMR spectra of 40% and 70% (w/w) M13 consist of a gaussian-shaped centerband surrounded by several similar sidebands (Fig. 1), in agreement with results reported for bacteriophage fd (DiVerdi and Opella, 1981). The linewidth $\Delta\nu_{1/2}$ of the centerband and the sidebands, defined as the full width at half-height, depends on the hydration of the gel and the temperature: at a ^{31}P NMR frequency of 202.5 MHz linewidths of 3.9, 3.2, 3.9 $\pm$ 0.2 ppm are found for 25%, 40%, and 70% M13 at 25°C and 4.0, 5.1, and 5.5 ppm for 18% M13 frozen at -40, -100, and -140°C, respectively (Fig. 2). For 40% M13, a linewidth of 2.7 $\pm$ 0.5 ppm is measured in the MAS NMR spectrum recorded at 121.5 MHz. The linewidth is independent of the spinning rate. By use of Herzfeld and Berger's sideband intensity tables (Herzfeld and Berger, 1980), MAS NMR spectra of 70% M13 at 25°C (Fig. 1) and 18% M13 frozen at -40°C (not shown) at various spinning rates can well be fitted by sideband patterns of a chemical shift tensor with relative tensor values $\sigma_{11} - \sigma_o = 77$,

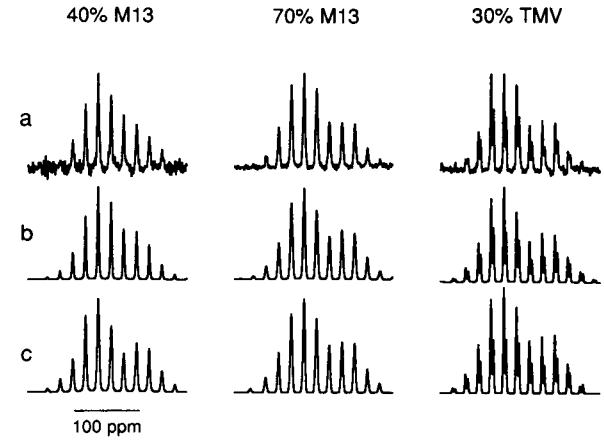

FIGURE 1 Experimental MAS NMR spectra of 40% M13 (128 scans) and 70% M13 (256 scans) and 30% TMV (20,000 scans) at 25°C (row *a*), simulated sideband patterns influenced by backbone motion (row *b*), and best "ideal" sideband fits (row *c*).

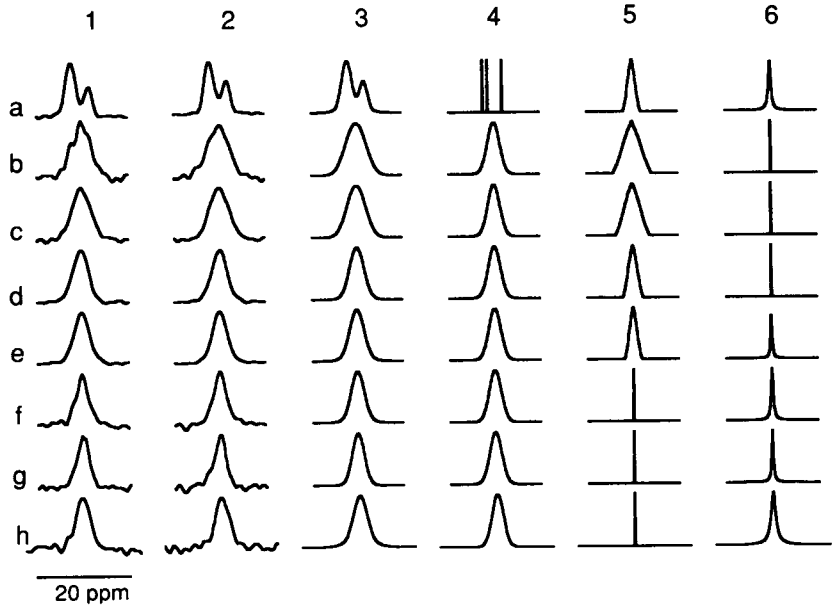

FIGURE 2 Experimental lineshape of the left first-order sideband (column *1*), average lineshape obtained by resampling the experimental MAS-free induction decay at multiples of the spinner rotation time after artificially increasing the time resolution by zero, filling in the spectral domain (column *2*) and simulated lineshapes (column *3*) consisting of a Φ contribution (column *4*), a θ_κ contribution (column *5*), and a contribution by homogeneous line broadening (column *6*), for 30% TMV (row *a*; 20,000 scans), 18% M13 at −140°C (row *b*; 10,000 scans), −100°C (row *c*; 10,000 scans) and −40°C (row *d*; 1,000 scans), 70% M13 (row *e*; 256 scans), 40% M13 (row *f*; 128 scans), 40% M13 at 121.5 MHz (row *g*; 1,000 scans) and 25% M13 (row *h*; 1,800 scans). Unless stated otherwise, experiments were conducted at 25°C and 202.5 MHz. The Φ contribution for TMV (row *a*; column *5*) also includes the effect of arginine binding (see text).

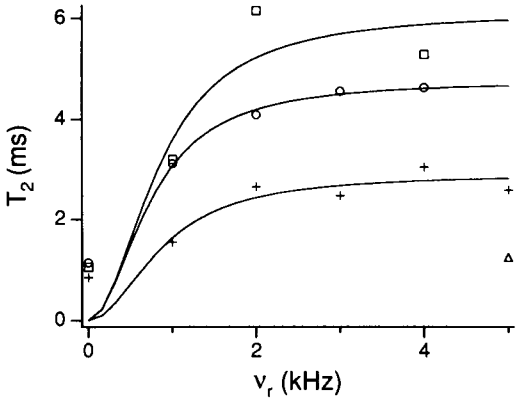

FIGURE 3 T_{2e} values obtained at various spinning rates for 70% M13 at 202.5 MHz (○), 40% M13 at 202.5 MHz (+), and 121.5 MHz (□) and 25% M13 at 202.5 MHz (△).

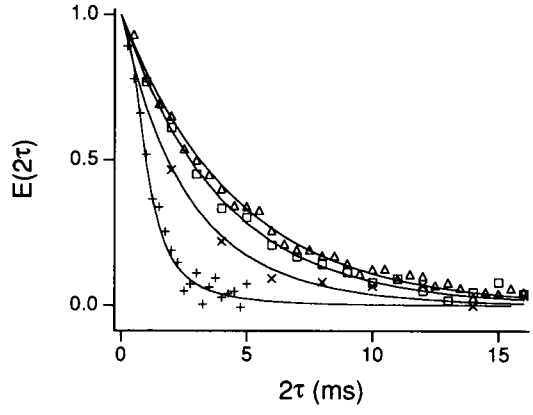

FIGURE 4 Transversal relaxation decay for 70% M13 at 202.5 MHz obtained at spinning rates of 0 kHz (+), 1 kHz (×), 2 kHz (□), and 4 kHz (△).

$\sigma_{22} - \sigma_o = 18$, and $\sigma_{33} - \sigma_o = -95 \pm 2$ ppm (Fig. 1 *c*). This agrees well with the values that have been estimated from the static lineshape at 202.5 MHz (not shown) and at 121.5 MHz (Magusin and Hemminga, 1993a). In contrast, spectra of 25% and 40% M13 at 25°C cannot be fitted by sideband patterns of a single chemical shift tensor (Fig. 1 *c*). Apparently, Herzfeld and Berger's theory does not apply for these cases.

At the ^{31}P NMR frequency of 202.5 MHz the MAS NMR spectrum of 30% (w/w) TMV shows two resolved sideband patterns with an overall intensity ratio of approximately 2:1 separated by 3.9 ± 0.3 ppm with a linewidth of 2.5 ± 0.3 ppm (Figs. 1 *a* and 2). The same intensity ratio and almost the same peak separation has been observed in the ^{31}P NMR spectrum of dry TMV at 121.5 MHz, but the linewidth at 121.5 MHz, 1.5 ppm, is less (Hemminga et al., 1987). The two sideband patterns can be compared with the "ideal" sideband patterns of static chemical shift tensors with various tensor values. The sideband pattern of a chemical shift tensor with relative tensor values $\sigma_{11} - \sigma_o = 79$, $\sigma_{22} - \sigma_o = 18$, and $\sigma_{33} - \sigma_o = -97 \pm 2$ ppm fits well to the pattern of major peak and a good fit to the minor peak pattern is obtained for a chemical shift tensor with tensor values 85, 18, and −103 ± 2 ppm (Fig. 1 *c*). These tensor values are slightly reduced as compared with the values obtained from MAS NMR spectra of dry TMV (Hemminga et al., 1987).

We have also investigated the transversal relaxation time T_{2e} of several M13 gels under MAS conditions (Fig. 3). In general, the centerband and sidebands decay exponentially as a function of the echo time and a T_{2e} value may be obtained by fitting a single exponential to each of these decays. No significant T_{2e} differences among the centerband and the sidebands have been found and the shape of the bands does not change at increasing echo time. T_{2e} values obtained at spinning rates greater than 2 kHz are systematically larger than those obtained from static experiments on the same samples and the value of T_{2e} is somewhere in between at a

rate of 1 kHz (Figs. 3 and 4). It was impossible to measure T_{2e} in the range of spinning rates less than 1 kHz, because the spinner rotation time became too long a sampling time with respect to T_{2e} to be measured. Similar to the outcome of nonspinning experiments, T_{2e} increases with decreasing water content and ^{31}P NMR frequency (Fig. 5). At 202.5 MHz, the T_{2e} values determined for the major and the minor peak in the 4-kHz MAS NMR spectrum of 30% TMV are 2.4 and 2.9 ms, respectively. Longitudinal ^{31}P NMR relaxation times T_1 of M13 gels at 202.5 MHz were generally in the order of seconds, thus three orders of magnitude larger than the T_{2e} values measured at high spinning rates.

DISCUSSION

Analysis of sideband intensities

As reported previously, ^{31}P NMR lineshapes and transversal relaxation of nonspinning samples of M13 and TMV cannot be interpreted consistently in terms of a single type of motion, like the rotation of the rod-shaped virions about their length axis alone. Instead, a fast type of restricted motion with a frequency greater than 10^5 Hz seems to be superimposed on the slow overall motion of the virions (Magusin and Hemminga, 1993a). The occurrence of motions can also explain the fact that Herzfeld and Berger's theory does not apply to the sideband intensities of dilute M13 gels. By analogy with motional narrowing under nonspinning conditions (Magusin and Hemminga, 1993b), it may be reasonably assumed that motions with frequencies less than 10^3 would not be able to significantly alter the sideband pattern caused by the ^{31}P chemical shift anisotropy with a "size" $(\omega_o/2\pi)\,|\,\sigma_{33} - \sigma_{11}\,|$ of 34 kHz at 202.5 MHz. In contrast, dramatic line-broadening effects would be expected for motions in the 10^3 Hz region, because their frequencies would be in the order of the spinning rates applied (Schmidt et al., 1986; Schmidt and Vega, 1987). As all M13 spectra recorded at various spinning rates, temperatures, and water contents contain well resolved sidebands, the motions that modify the sideband intensities should therefore have frequencies greater than 10^4 Hz.

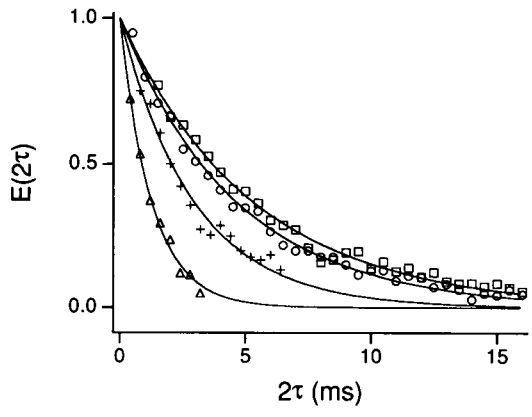

FIGURE 5 Transversal relaxation decay at spinning rates of 4 kHz for 70% M13 at 202.5 MHz (○), 40% M13 at 202.5 MHz (+), and 121.5 MHz (□); decay of 25% M13 at 202.5 MHz at a rate of 5 kHz (△).

To extract motional information from the sideband pattern more quantitatively, the previously used model (Magusin and Hemminga, 1993b), in which the fast motions of the nucleic acid phosphodiesters are collectively described as restricted rotation about the virion length axis, is extended to MAS NMR experiments (Eq. 2). Quickly summarizing our previous discussion (Magusin and Hemminga, 1993a), we do not wish to pretend that uniaxial rotation about the viral axis is a realistic model for the various types of backbone motion that the nucleic acid molecule inside M13 or TMV may undergo simultaneously. Judging from the complex dynamics observed for "naked" nucleic acids in solution (Alam and Drobny, 1991), we actually believe that, as a result of steric constraints and concerted motions, the dynamics of the nucleic acids encapsulated in TMV and M13 are likely to be much more complicated. By employing the uniaxial diffusion model we simply want to characterize the spatial restriction of nucleic acid backbone motion by a single "cumulative amplitude" λ, much like the general order parameter S used in Model Free analyses of relaxation measurements to characterize the amount of motional anisotropy (Lipari and Szabo, 1982a; 1982b). In fact, the functions $\mathrm{sinc}(\lambda)$ and $\mathrm{sinc}(2\lambda)$ in Eq. 2 can be shown playing a role similar to S in the (simplified) autocorrelation functions (see Appendix). In our opinion, a more realistic model for nucleic acid backbone motion would involve too many parameters, which would lead to overinterpretation of the experimental data or require additional, questionable assumptions. This would especially be the case for M13, because hardly anything is known about the geometry of its internal DNA molecule. For M13, the nonspecific character of our simple model is actually enhanced by the assumption that the phosphodiesters are randomly oriented within the virus particles, which themselves are randomly oriented within the gel. As long as no correlation between the orientation of the phosphodiesters and the local axes of backbones motion exists and the effect of slow overall motion about the length axis of the virus is negligible, our model describing phosphodiester motion in terms of uniaxial motion about the viral axis, is theoretically equivalent to any other model that involves uniaxial diffusion about one or more axes not parallel to the viral axis.

Sideband patterns calculated using Eq. 2 for restriction half-angles λ equal to multiples of 9° between 0° and 90°, have been compared with various ^{31}P MAS NMR spectra of M13. Spectra simulated for $\lambda = 27° \pm 5°$ fit well to MAS NMR spectra of 40% M13 at 202.5 MHz at spinning rates of 4 and 5 kHz (Fig. 1) and almost the same λ value, $36° \pm 5°$, produces the best fit to the 4-kHz MAS NMR spectrum of the same gel at 121.5 MHz. The 4-kHz MAS NMR spectrum of 70% M13 at 202.5 MHz is best reproduced for $\lambda = 9°$, and a λ value of 45° is extracted from the 5-kHz MAS NMR spectrum of 25% M13 at 202.5 MHz. These restriction half-angles agree with the values of 27° and 0° obtained by simulating the nonspinning ^{31}P NMR lineshape of the 40% and 70% M13 sample at 202.5 MHz (not shown) and are also consistent with the values 52° and 43° obtained by analysis

of nonspinning lineshapes of 15% and 30% M13 at 121.5 MHz (Magusin and Hemminga, 1993a). A relation may exist between the increase of motional amplitude and the swelling of M13 at increasing hydration (Dunker et al., 1974). At increasing diameter of the hollow tube inside the rod-shaped phage, nucleic acid backbone motion may increase by the reduction of steric hindrance. When comparing the λ value of about 30° obtained for 40% M13 gels with, for example, backbone fluctuations of $\pm 27°$ in the gigahertz range reported earlier for DNA (Hogan and Jardetzky, 1980), it should be realized that our model is presumably too simple. Diffusion models involving more angle fluctuations would probably result in smaller restriction angles per fluctuating angle than the λ values found above. Recently, we could further improve the simulated ^{31}P NMR powder lineshapes of M13 at 121.5 MHz by assuming that the backbone of M13 DNA consists of 83% immobile and 17% mobile phosphodiesters. A similar, 5:1 two-component model produces a better simulation of the nonspinning spectrum of 40% M13 at 202.5 MHz as well (not shown), but the two-component model does not significantly improve the simulated MAS NMR spectra.

For TMV, a three-component model is reasonable, because three sets of binding sites exist within the virion. Nonspinning ^{31}P NMR lineshapes of 30% TMV provide strong indications that one of these three sets is more mobile than the other two, but the question which the mobile set is, cannot be solved unambiguously due to the overlap of their broad powder lines (Magusin and Hemminga, 1993a). The fact that one of the three resonance lines in ^{31}P NMR spectra of oriented TMV solutions is much broader than the other two, indicates a high level of disorder for one of the three sets of phosphodiesters in TMV (Cross et al., 1983a), which seems to support our conclusion that one of the three sets of phosphodiesters is less rigidly bound. Cross et al. have speculatively assigned this resonance line to a specific binding site labeled 3 in the computer-refined crystal structure presented by Stubbs and Stauffacher (1981). Using this structure we have recalculated the chemical shift positions of the resonance lines in the oriented spectrum, however, and differently assigned the broad line to site 2 (Magusin and Hemminga, 1993a). Given the ambiguity in the spectral assignment, the question of which binding site could actually be less rigidly bound still remains to be answered.

Because MAS NMR spectra of TMV show two resolved, potentially motion-affected sideband patterns, they offer an extra possibility for assigning mobility to the three sites more specifically. Interpretation of the two sideband patterns in terms of "ideal" MAS behavior shows that the apparent chemical shift anisotropy of the minor resonance is larger than the anisotropy of the major resonance. This was also found for dried TMV samples (Hemminga et al., 1987) and can be observed in the MAS NMR spectrum of 10% TMV solution (Cross et al., 1983a) as well, although this effect was not mentioned in the text of this paper. Taking bond angle and arginine binding effects into account, we assign the minor sideband pattern to site 1, as labeled by Stubbs and Stauffacher (1981), and the major sideband pattern to sites 2 and 3 (see Analysis of Lineshapes). The fact that the apparent anisotropy of the major resonance is reduced relative to the minor resonance would then be consistent with our hypothesis to be discussed in Analysis of Lineshapes, that site 2 is less rigidly bound than the other two.

Indeed, a three-component simulation using Eq. 2 produces a good fit, when identical tensor values of 83, 25, and -108 ppm are assumed for the three sites and restriction half-angles are taken as 18°, 45°, and 18° for sites 1, 2, and 3, respectively (Fig. 1). These values may be compared with the respective half-angles 9°, 86°, and 17° obtained from the analysis of the nonspinning ^{31}P NMR lineshape of another sample of 30% TMV at 121.5 MHz (Magusin and Hemminga, 1993a). The difference between these two sets of angular amplitudes shows the difficulty of extracting motional parameters for each site separately from nonspinning spectra due to the strong overlap of their resonances. The presence of motional narrowing in nonspinning and MAS NMR spectra of 30% TMV recorded at 121.5 and 202.5 MHz, respectively, is difficult to reconcile with the absence thereof in spectra of 10% TMV solutions at 60.9 MHz (Cross et al., 1983a). This may be caused by differences in the methods employed by Cross et al. to prepare TMV samples and record their spectra. Because the NMR spectrum-recording method is insufficiently described in their paper, a more specific explanation would only be highly speculative.

Analysis of transversal relaxation

The observed dependence of T_{2e} on the spinning rate less than 2 kHz (Fig. 3) indicates a contribution by slow phosphodiester reorientation to transversal relaxation. Because T_{2e} becomes shorter as the M13 gel becomes more fluid, we tentatively assign this slow phosphodiester reorientation to the overall rotation of the rod-shaped virus particles about their length axis. At spinning rates greater than 2 kHz, T_{2e} approaches an upper limit, indicating that another relaxation mechanism, which is independent of the spinning rate, becomes more important. Other features of this relaxation mechanism are that it is sensitive to hydration and depends on the magnetic field strength (Figs. 3 and 5). In principle, the observed T_{2e} increase at decreasing hydration (Table 1) could simply result from the removal of mobile water protons in the vicinity of ^{31}P, because water protons could increase ^{31}P relaxation by causing fast fluctuating dipolar interactions. Such ^{1}H-^{31}P dipolar contribution to longitudinal and transversal ^{31}P relaxation may be estimated by using general equations presented elsewhere (Wittebort and Szabo, 1978). As learned from these equations, the fact that T_1 is three orders of magnitude larger than T_2, as observed in our experiments, is typical for motions with frequencies which are one or two orders of magnitude lower than the angular resonance frequencies of ^{31}P and ^{1}H. Indeed, transversal relaxation of ^{31}P nuclei by protons which undergo motions in this frequency range (10^7–10^8 Hz) is not affected by the 30-kHz proton decoupling used in our experiments. The general

TABLE 1 Restriction half-angles and diffusion coefficients for local backbone motion of the DNA molecule inside M13 and the influence of backbone motion on the homogeneous and the inhomogeneous linewidth.

[M13]	ν_o	λ	T_{2e}	D'_{app}	T_{2e}^{CSA}	D'	$\Delta\nu_{1/2}$	$\Delta\nu_{hom}$	$\Delta\nu_{inh}$
%	(MHz)	(°)	(ms)	(kHz)	(ms)	(kHz)	(Hz)	(Hz)	(Hz)
70	202.5	9 ± 5	4.6	40	6.8	60 ± 50	780	70	710
40	202.5	30 ± 5	3.0	250	3.5	300 ± 80	640	105	535
40	121.5	30 ± 5	5.3	190	9.8	300 ± 80	330	60	270
25	202.5	45 ± 5	1.3	210	1.4	240 ± 40	780	250	530

[M13], weight fraction of M13 in the gel; ν_o, ^{31}P NMR frequency; λ, restriction half-angle for local backbone motion derived from the sideband pattern; T_{2e}, relaxation time for the part of transversal relaxation that is independent of the spinning rate; D'_{app}, apparent diffusion coefficient calculated from T_{2e} by using Eq. 7; T_{2e}^{CSA}, transversal relaxation time due to fast phosphodiester reorientation, calculated from T_{2e} by correcting for an additional ν_o independent T_{2e}^{DIP} of 16 ms; D', diffusion coefficient calculated from T_{2e}^{CSA} by using Eq. 7; $\Delta\nu_{1/2}$, full linewidth at half-height of the centerband and the sidebands; $\Delta\nu_{hom}$, homogeneous linewidth; $\Delta\nu_{inh}$, inhomogeneous linewidth.

equations, however, also predict T_{2e} to be independent of the magnetic field strength in this frequency range and thus fail to explain the difference between the T_{2e} values measured for 40% M13 at 121.5 and 202.5 MHz.

Alternatively, the same fast backbone motions that are responsible for the motional modification of the sideband intensities, could also cause transversal relaxation due to the chemical shift anisotropy of the ^{31}P nuclei. Such relaxation mechanism would provide a qualitative explanation for the observed dependence on the magnetic field. As noticed under Analysis of Sideband Intensities, hydration affects the amplitude of nucleic acid backbone motions, which could explain qualitatively the observed T_{2e} trend at increasing hydration. Assuming that phosphodiester reorientation by slow, overall rotation of the virion and by fast restricted backbone motion is the main cause of transversal relaxation, we have used Eq. 8 to explain the observed dependence of T_{2e} on the spinning rate. Indeed, sigmoid curves, as predicted by Eq. 8, fit well to the T_{2e} values obtained for spinning rates of 1 kHz and higher at 202.5 MHz and reasonably to T_{2e} values measured at 121.5 MHz (Fig. 3). Obviously, the model fails to predict correct T_{2e} values for static samples. This is due to the assumption implicit in Eq. 5 that the decay of echoes is sampled at even multiples of the rotation time T_r, which goes to infinity as the spinning rate drops to zero.

Diffusion coefficients D for the rotational diffusion of the virus particles about their length axis may be estimated from the best fits in Fig. 3 and the half-angles λ estimated from the sideband intensities (see Analysis of Sideband Intensities). Using λ values of 9° and 30° for 70% and 40% M13, we find D values of 1.4 and 4.4 Hz for 70% and 40% M13 at 202.5 MHz and 5.2 Hz for 40% M13 at 121.5 MHz, respectively. These values are mutually consistent within experimental error and also agree with the values reported previously for 15% and 30% M13 gels (Magusin and Hemminga, 1993a). The ω_r-independent part of transversal relaxation may also be estimated from the curves in Fig. 3. For example, for 70% M13, this part of transversal relaxation is characterized by a T_{2e} value of 4.8 ms. Actual echo decays simulated by multiplication of Eq. 5 for D = 1.4 Hz and an exponential decay with T_{2e} = 4.8 ms fit well to the experimental decays obtained for 70% M13 at the spinning rates applied (Fig. 4). Apparently, the multiexponential decay in Eq. 5 is indeed reasonably approximated by a single exponential with relaxation time T_{2e}^{SOR} as described by Eq. 6. The static relaxation decay measured for 70% M13, can also be simulated for D = 1.4 Hz by using a previously discussed model (Magusin and Hemminga, 1993b). This shows that the outcome of spinning and nonspinning relaxation experiments can be interpreted consistently in terms of our models. The ratio between the static T_{2e} values 1.06 and 0.85 ms at 121.5 and 202.5 MHz closely approximates 1.4, as expected from the $(\omega_o)^{-2/3}$ dependence of transversal relaxation by ultraslow diffusion under nonspinning conditions (Magusin and Hemminga, 1993b).

From the ω_r-independent part of transversal relaxation, an apparent diffusion coefficient D'_{app} for the fast phosphodiester reorientation can be calculated directly by using Eq. 7. Different D'_{app} values, however, are found for 40% M13 at 121.5 and 202.5 MHz in this way (Table 1). This inconsistency may be eliminated by also taking into account another relaxation mechanism, which is independent of both ω_r and ω_o. Such a type of relaxation could be caused by fluctuating dipolar interactions between ^{31}P and other nuclei in its vicinity, like ^{1}H, ^{14}N, or other ^{31}P nuclei. For 40% M13, the ω_r-independent T_{2e} values 6.1 and 2.9 ms determined at 121.5 and 202.5 MHz could result from a ω_o-independent contribution T_{2e}^{DIP} of 16 ms superimposed on T_{2e}^{CSA} values of 9.8 and 3.5 ms, respectively. Similarly, we derived T_{2e}^{CSA} from the spinning rate independent T_{2e} values of 70% and 25% M13 gels, assuming T_{2e}^{DIP} to be the same. The diffusion coefficients D' which follow from these "corrected" T_{2e}^{CSA} values by using Eq. 7 are in the order of 10^5 Hz (Table 1). D' values determined for 25% and 40% M13 are the same within the error caused by the ±5° uncertainty in λ, indicating that in this concentration range the amplitudes of the backbone motions are more sensitive to small hydration changes than their frequencies. More extreme dehydration, however, also influences the frequency of backbone motions, as illustrated by the lower D' value found for 70% M13. The finding that the major peak in the MAS NMR spectrum of TMV decays faster than the minor peak indicates that the average mobility of the two binding sites giving rise to the major peak, is larger than the mobility of the binding site causing the minor peak. This is consistent with the λ values obtained from the sideband pattern in the previous section.

The effective diffusion coefficient D' determined by using our simple model is only a qualitative measure which indi-

cates if the backbone motions dominating transversal relaxation at spinning rates greater than 2 kHz become faster or slower under varying conditions. Its value may not even be realistic by order of magnitude, e.g., when the cumulative amplitude λ actually reflects several types of backbone motion, whereas transversal relaxation is dominated by only the slowest one. However, a minimum and a maximum order of magnitude may be estimated from relaxation measurements. On the one hand, the invariance of T_{2e} at different spinning rates between 2 and 5 kHz, shows that the backbone motions dominating transversal relaxation at these rates are in the order of 10^4 Hz or faster. On the other hand, the three orders of magnitude difference between T_1 and T_{2e} at ^{1}H and ^{31}P resonance frequencies in the order of 10^9 rad/s, sets an upper limit of 10^7–10^8 Hz, as may be estimated from more general equations presented elsewhere (Wittebort and Szabo, 1978).

Analysis of lineshapes

Line broadening caused by sample preparation has been suggested as an explanation for the large MAS NMR linewidths generally observed for dried and lyophilized biological materials as compared with solution linewidths (Hemminga et al., 1987). Indeed, it is conceivable, that as a consequence of the dehydration process, the material partly decomposes, or susceptibility heterogeneity is introduced. Such effects, however, are less likely explanations for the broad lines observed for M13 samples frozen at temperatures of −140°C and less, because these are homogeneous lumps of ice pressed rigidly against the inner wall of the MAS spinner. At a macroscopic level, there are no visible differences between M13 ice at −40°C and −140°C, nor do the tuning properties of M13 samples change greatly on changing the temperature between those values, indicating that no phase transition occurs in this temperature trajectory. Nevertheless, the linewidth strongly increases as the sample is cooled down from −40°C to −140°C. It has been suggested that the difference between the shift position of the major and the minor peak in ^{31}P MAS NMR spectra of TMV reflects conformational differences among the three types of binding sites (Hemminga et al., 1987). Because the ^{31}P MAS NMR linewidth measured for M13 at −140°C and less is comparable with the isotropic shift range observed for TMV at room temperature (Fig. 2), a spread of static phosphodiester conformations in a similar range as in TMV could offer a possible explanation for the observed M13 lineshape. At higher temperatures the linewidth in MAS NMR spectra of M13 is less. It gradually decreases to a minimum value of 3.0 ppm as the sample becomes more fluid and the amount of internal DNA backbone motion within the virions increases, going from frozen samples at −100°C and −40°C to viscous gels of 70% and 40% M13 at 25°C. Apparently, the isotropic shift range becomes narrower as temperature or hydration increases.

Beside influencing the sideband intensities and transversal relaxation by their reorientational character, fast backbone motions could also cause fast fluctuation of the phosphodiester conformations, which may lead to "conformational averaging" of the isotropic shift. Such conformational averaging due to nucleic backbone motions could offer a possible explanation for the reduction of the linewidth at increasing hydration and temperature. In contrast, transversal relaxation tends to broaden the centerband and the sidebands at increasing hydration by adding an increasing homogeneous linewidth to the inhomogeneous linewidth. Indeed, the increased linewidth observed for 25% M13 gels, as compared with 40% M13, could be caused mainly by the increased homogeneous linewidth alone, superimposed on an inhomogeneous width of 2.7 ppm (Table 1).

To test the hypothesis that a distribution of phosphodiester conformations underlies the observed gaussian lineshapes observed in ^{31}P MAS NMR spectra, the lineshapes of the centerband and the sidebands in MAS NMR spectra of M13 have been simulated by use of Eq. 9, which takes into account a spread of values for the two types of angles that affect the isotropic shift most strongly, i.e., the RO-P-OR′ bond angles Φ, supposed to be static in our model, and the dihedral angles θ_1 and θ_2, assumed to be quickly fluctuating. Homogeneous line broadening is added as a third broadening factor (Fig. 2). The five model parameters involved in the simulation cannot be unequivocally determined from the measured lineshapes alone, and external arguments are necessary to estimate their values. For the lineshapes at 25°, the homogeneous linewidth $1/\pi T_{2e}$ is calculated from T_{2e} measured at spinning rates of 4 and 5 kHz (Fig. 3). For the frozen M13 samples, homogeneous line broadening is neglected. As mentioned under Theory, the static θ_κ distribution parameter v is taken as 20°, which represents a realistic spread of dihedral angles in various phosphodiester compounds (Giessner-Prettre et al., 1984). For parameter G, the isotropic chemical shift change per unit bond angle change, we use a value of 2 ppm per degree, as indicated by empirical data (Gorenstein, 1981). Because the observed linewidth reaches a minimum for 40% M13, we assume the θ_κ contribution to be completely averaged at this hydration, so that a gauss fit to the lineshape that is left after deconvolution with the homogeneous line directly provides the static Φ distribution parameter w as 0.9° (Fig. 2), which seems realistic as compared with the 3° range of Φ in TMV. In contrast, the lineshape at −140°C is assumed to be completely static, from which the dihedral shift range parameter b may be estimated to be −2.0 ppm, in agreement with the range of 3.2–3.8 ppm calculated for the θ_κ contribution to the isotropic shift (Giessner-Prettre et al., 1984). With these parameter values, we obtain good fits for 18% M13 at −100°C and −40°C and 70% M13 at 25°C, for restriction half-angles μ of 17°, 37°, and 40°. When interpreting these large μ values it should be realized that the description of conformational fluctuations in terms of only the two dihedral angles θ_κ is probably too simple. A more sophisticated model with more fluctuating conformational parameters would probably result in smaller restriction angles per parameter. The μ values found above should probably be regarded most safely as upper limits rather than as realistic values. Furthermore, factors other than conformational averaging may play a role in the observed effect of

temperature and hydration on the MAS NMR lineshape. Conformational averaging is only a possible explanation, but not the only one. Comparison of the restriction angles estimated from the lineshapes and the sideband intensities above seems to indicate that under conditions which suppress phosphodiester reorientation, e.g., in frozen samples at −40°C, some of the conformational parameters may still fluctuate considerably .

Recently, the major and the minor sideband pattern in the MAS NMR spectrum of TMV were assigned on the basis of the $C_{3'}$-$O_{3'}$-P-$O_{5'}$ and $O_{3'}$-P-$O_{5'}$-$C_{5'}$ torsional angles (Hemminga et al., 1987). An alternative assignment, however, can be made if the RO-P-OR′ bond angles Φ are taken into account, to which the isotropic chemical shift of phosphodiesters is more sensitive (Gorenstein, 1981). A bond angle increase of only 5° already causes the isotropic shift to decrease 7 ppm (Giessner-Prettre et al., 1984). Because Φ is 103°, 103°, and 100° for sites 1, 2, and 3, respectively, as calculated from model coordinates (Stubbs and Stauffacher, 1981), we would expect the occurrence of a major peak belonging to sites 1 and 2, about 4 ppm upfield of a minor peak belonging to site 3 (Fig. 6 *b*). Because this does not agree with the observed spectrum (Fig. 6 *a*), even if torsional angle effects of about 1.5 ppm would be involved as well, we have also taken the influence of arginine bonding into account.

In RNA-protein interaction models for TMV, two sites are generally interacting closely with arginine residues, whereas no arginine is close to a third one. The less bound site, however, seems to be assigned differently in different papers. For example, in the paper of Stubbs et al. (1977) it is site 2 (taking into account a change of labels between sites 1 and 2 as compared with our labeling, which follows other papers (Stubbs and Stauffacher, 1981; Namba and Stubbs, 1986)), whereas in the model of Namba and Stubbs in 1986 site 3 is the one without close arginine contact. Similar to the effect caused by binding of a water molecule to a phosphodiester group (Ribas Prado et al., 1979), a 3.5-ppm decrease of the isotropic shift could be expected due to arginine-phosphate interaction. Assuming on the one hand, that sites 1 and 2 are tightly bound to arginine residues, the spectrum predicted above on the basis of Φ differences alone, should be modified by shifting the major peak even 3.5 ppm further upfield. This would increase the predicted separation between the minor and the major peak to 7.5 ppm, and their shift order would still disagree with the experimental spectrum (Fig. 6 *c*). If, on the other hand, sites 1 and 3 were bound, the resonances belonging to sites 1 and 3 would shift 3.5 ppm upfield, so that resonance of site 3 would be located 0.5 ppm downfield of the position of site 2 (Fig. 6 *d*). The resulting spectrum would agree with the experimental spectrum by containing a major peak belonging to the overlapping resonances of site 2 and 3, about 3.8 ppm downfield of a minor peak belonging to site 1. It should be noticed that such assignment is only speculative, because the effect of arginine binding on the isotropic chemical shift of ^{31}P inside TMV is unknown and other factors, not accounted for in our model, can also influence the isotropic chemical ^{31}P shift. The supposed absence of close contacts between site 2 and an arginine residue, however, would be consistent with our earlier suggestion that this site is more mobile than the other two (Magusin and Hemminga, 1993a). This is also confirmed by our analysis of the sideband patterns and transversal relaxation of the two peaks.

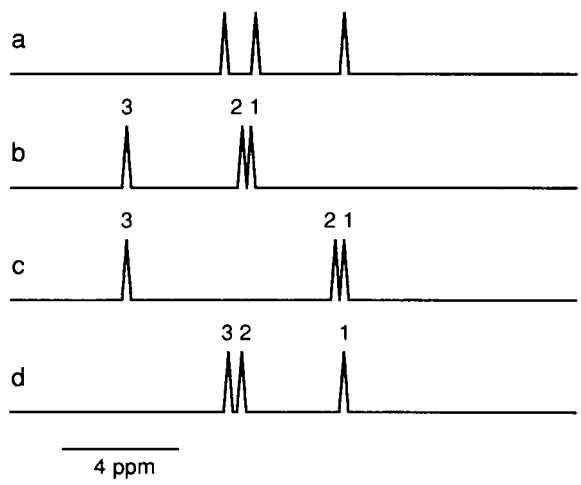

FIGURE 6 Stick spectra illustrating the assignment of the peaks in MAS NMR spectra of TMV; unassigned stick spectrum derived from the experimental lineshape (*a*), hypothetical spectrum based on the Φ angle effects only (*b*), spectra also taking arginine binding into account to either sites 1 and 2 (*c*) or sites 1 and 3 (*d*).

Recently, we reported that in MAS NMR spectra of lyophilized TMV samples, the major and minor sideband patterns are not resolved (Hemminga et al., 1987). A possible explanation for this effect is provided by our model. The absence of conformational averaging of the isotropic chemical shift at extremely low hydration probably spoils the resolution of the peaks in the MAS NMR spectrum of lyophilized TMV, much like the broad peak observed for frozen M13 samples at −140°C. Using the M13 model parameters ν = 20° and b = −2.0 ppm for 30% TMV at 25° as well, and taking a homogeneous linewidth of 130 Hz for both peaks, a good fit to the major and minor peak is obtained for μ = 40°, if the resonances of sites 2 and 3 are assumed to be located 3.1 and 4.2 ppm downfield of the resonance of site 1, respectively (Fig. 2).

CONCLUSION

The model of phosphodiester motion in gels of M13 and TMV, which recently emerged from analyses of ^{31}P NMR lineshapes and transversal relaxation of static NMR samples (Magusin and Hemminga, 1993a), is also consistent with the effects of motion on sideband spectra and transversal relaxation under MAS conditions. Overall rotation of the rod-shaped virions about their length axis and local backbone motions of the encapsulated nucleic acid molecules are responsible for the various deviations from "ideal" MAS behavior. Sideband intensities seem to be influenced by fast restricted reorientation of the phosphodiester groups, caused by nucleic acid backbone motions. Sideband patterns and

transversal relaxation observed for 25% and 40% M13 are consistent with angular amplitudes of 30° and 45°. These amplitudes should be regarded as cumulative motional parameters of whole classes of motions, rather than as realistic amplitudes of specific motions alone, because the description of the complicated backbone dynamics as only one type of uniaxial diffusion is probably too simple. The increase of motional amplitudes at increasing hydration could perhaps be related to swelling of the M13 virions. Effective frequencies of the backbone motions in the order of 10^5 kHz can be estimated from the spinning rate independent part of transversal relaxation, which is measured at spinning rates above 2 kHz, but these values can hardly be related to actual microscopic rate constants due to the cumulative character of the model. By causing the conformation of the phosphodiester groups to fluctuate, fast restricted backbone motions could also offer a possible explanation for the observed narrowing of the centerband and sidebands at high temperatures and hydration. Slow rotation of the virus particles about their length axis only contributes significantly to transversal relaxation at spinning rates less than 2 kHz. This contribution even becomes dominant under nonspinning conditions, which further justifies the neglect of other relaxation mechanisms in our analysis of nonspinning relaxation measurements (Magusin and Hemminga, 1993a).

This research was supported by the Netherlands Foundation of Biophysics with financial aid of the Netherlands Organization for Scientific Research (NWO). We are grateful to Gerda Nachtegaal and Leon ter Beek for experimental assistance, to Arno Kentgens for his program to analyze "ideal" sideband patterns, and to Johan Kijlstra for his survey of the literature about ^{31}P isotropic chemical shifts. We are especially indebted to the SON solid-state NMR facility in Nijmegen (the Netherlands), where the MAS NMR experiments were conducted.

APPENDIX: COMPARISON OF THE CUMULATIVE MOTIONAL AMPLITUDE λ AND THE GENERAL ORDER PARAMETER S

The description of the complex dynamic behavior of the encapsulated backbone using a nonspecific "cumulative amplitude" λ as a measure of the spatial restriction of the motion may be compared with the use of the generalized order parameter S in the Model Free analysis of longitudinal and transversal relaxation times (Lipari and Szabo, 1982a). In the Model Free approach S is defined as the limiting value S^2 of the simple correlation function for internal motion $C_I(t) = S^2 + (1 - S^2)\exp(-t/\tau_c)$ as $t \to \infty$. Similarly, in our combined diffusion model the sinc functions in Eq. 2 also appear in the limiting values $\mathrm{sinc}^2(\lambda)$ and $\mathrm{sinc}^2(2\lambda)$ for the correlation functions

$$\tfrac{5}{2}\langle D^2_{n1}(\Omega(0))[D^2_{n1}(\Omega(t))]^*\rangle$$

and

$$\tfrac{5}{2}\langle D^2_{n2}(\Omega(0))[D^2_{n2}(\Omega(t))]^*\rangle.$$

Like S^2, $\mathrm{sinc}^2(\lambda)$ and $\mathrm{sinc}^2(2\lambda)$ approximate 1 in the case of extremely limited motion ($\lambda \approx 0$) and vanish if the motion is unrestricted ($\lambda = \pi$).

REFERENCES

Alam, T. M., and G. P. Drobny. 1991. Solid-state NMR studies of DNA structure and dynamics. *Chem. Rev.* 91:1545–1590.

Banner, D. W., C. Nave, and D. A. Marvin. 1981. Structure of the protein and DNA in fd filamentous bacterial virus. *Nature.* 289:814–816.

Cross, T. A., S. J. Opella, G. Stubbs, and D. L. D. Caspar. 1983a. Phosphorus-31 nuclear magnetic resonance of the RNA in tobacco mosaic virus. *J. Mol. Biol.* 170:1037–1043.

Cross, T. A., P. Tsang, and S. J. Opella. 1983b. Comparison of protein and deoxyribonucleic acid backbone structures in fd and Pf1 bacteriophages. *Biochemistry.* 22:721–726.

DiVerdi, J. A., and S. J. Opella. 1981. Phosphorus-31 nuclear magnetic resonance of fd virus. *Biochemistry.* 20:280–284.

Dufourc, E. J., C. Mayer, J. Stohrer, G. Althoff, and G. Kothe. 1992. Dynamics of phosphate head groups in biomembranes. Comprehensive analysis using phosphorus-31 nuclear magnetic resonance lineshape and relaxation time measurements. *Biophys. J.* 61:42–57.

Dunker, A. K., R. D. Klausner, D. A. Marvin, and R. L. Wiseman. 1974. Filamentous bacterial viruses X. X-ray diffraction studies of the R4 A-protein mutant. *J. Mol. Biol.* 81:115–117.

Edmonds, A. R. 1960. Angular Momentum in Quantum Mechanics. Princeton University Press, Princeton, NJ. 146 pp.

Giessner-Prettre, C., B. Pullman, and F. Ribas Prado. 1984. Contributions of the PO Ester and CO torsion angles of the phosphate group to ^{31}P-nuclear magnetic shielding. *Biopolymers* 23:377–388.

Gorenstein, D. G. 1981. Nucleotide conformational analysis by ^{31}P nuclear magnetic resonance spectroscopy. *Annu. Rev. Biophys. Bioeng.* 10: 355–386.

Haeberlen, U. 1976. High Resolution NMR in Solids: Selective Averaging. Academic Press, New York. 208 pp.

Hemminga, M. A., P. A. De Jager, J. Krüse, and R. M. J. N. Lamerichs. 1987. Magic-angle-spinning NMR on solid biological systems. Analysis of the origin of the spectral linewidths. *J. Magn. Reson.* 71:446–460.

Herzfeld, J., and A. E. Berger. 1980. Sideband intensities in NMR spectra of samples spinning at the magic angle. *J. Chem. Phys.* 73:6021–6030.

Hogan, M. E., and O. J. Jardetzky. 1980. Internal motions in deoxyribonucleic acid II. *J. Am. Chem. Soc.* 19:3460–3468.

Lipari, G., and A. Szabo. 1982a. Model-free approach to the interpretation of nuclear magnetic resonance relaxation in macromolecules. 1. Theory and range of validity. *J. Am. Chem. Soc.* 104:4546–4559.

Lipari, G., and A. Szabo. 1982b. Model-free approach to the interpretation of nuclear magnetic resonance relaxation in macromolecules. 2. Analysis of experimental results. *J. Am. Chem. Soc.* 104:4559–4570.

Magusin, P. C. M. M., and M. A. Hemminga. 1993a. Analysis of ^{31}P NMR lineshapes and transversal relaxation of bacteriophage M13 and Tobacco Mosaic Virus. *Biophys. J.* 64:1861–1868.

Magusin, P. C. M. M., and M. A. Hemminga. 1993b. A theoretical study of rotational diffusion models for rod-shaped viruses: the influence of motion on ^{31}P NMR lineshapes and transversal relaxation. *Biophys. J.* 64:1851–1860.

Marvin, D. A., R. L. Wiseman, and E. J. Wachtel. 1974. Filamentous bacterial viruses XI. Molecular architecture of the class II (Pf1, Xf) virion. *J. Mol. Biol.* 82:121–138.

Mehring, M. 1983. Principles of High Resolution NMR in Solids. Springer-Verlag, Berlin. 342 pp.

Namba, K., and G. Stubbs. 1986. Structure of tobacco mosaic virus at 3.6 Å resolution: implications for assembly. *Science* 231:1401–1406.

Pauls, K. P., A. L. MacKay, O. Söderman, M. Bloom, A. K. Tanjea, and R. S. Hodges. 1985. Dynamic properties of the backbone of an integral membrane polypeptide measured by deuteron NMR. *Eur. Biophys. J.* 12:1–11.

Ribas Prado, F., C. Giessner-Prettre, B. Pullman, and J.-P. Daudey. 1979. Ab initio quantum mechanical calculations of the magnetic shielding tensor of phosphorus-31 of the phosphate group. *J. Am. Chem. Soc.* 101: 1737–1742.

Schmidt, A., S. O. Smith, D. P. Raleigh, J. E. Roberts, R. G. Griffin, and S. Vega. 1986. Chemical exchange effects in NMR spectra of rotating solids. *J. Chem. Phys.* 85:4248–4253.

Schmidt, A., and S. Vega. 1987. NMR line shape analysis for two-site exchange in rotating solids. *J. Chem. Phys.* 87:6895–6907.

Slichter, C. P. 1978. Principles of Magnetic Resonance. Springer-Verlag, Berlin. 397 pp.

Stubbs, G., and C. Stauffacher. 1981. Structure of the RNA in tobacco mosaic virus. *J. Mol. Biol.* 152:387–396.

Stubbs, G., S. Warren, and K. Holmes. 1977. Structure of RNA and RNA binding site in tobacco mosaic virus from 4 Å map calculated from x-ray fiber diagrams. *Nature.* 267:216–221.

Thomas, G. J., Jr., B. Prescott, S. J. Opella, and L. A. Day. 1988. Sugar pucker and phosphodiester conformations in viral genomes of filamentous bacteriophages: fd, If1, IKe, Pf1, Xf, and Pf3. *Biochemistry.* 27: 4350–4357.

Wittebort, R. J., and A. J. Szabo. 1978. Theory of NMR relaxation in macromolecules: restricted diffusion and jump models for multiple internal rotations in amino acid side chains. *J. Chem. Phys.* 69: 1722–1736.